

# (Pentamethylcyclopentadienyl)iridium Polyhydride Complexes: Synthesis of Intermediates in the Mechanism of Formation of $(C_5(CH_3)_5)IrH_4$ and the Preparation of Several Iridium(V) Compounds

Thomas M. Gilbert, Frederick J. Hollander, and Robert G. Bergman\*

Contribution from the Department of Chemistry, University of California, and Materials and Molecular Research Division, Lawrence Berkeley Laboratory, Berkeley, California 94720.  
Received October 17, 1984

**Abstract:** Reaction of  $LiBH_4$  with  $[(C_5(CH_3)_5)Ir]_2(\mu-H)_3PF_6$  (**1**) results in the formation of the borohydride-bound dimer  $[(C_5(CH_3)_5)Ir]_2H_3BH_4$  (**2**, R = H), for which a single-crystal X-ray diffraction study shows the borohydride moiety bridging the two metal centers in a unique fashion. Hydrolysis of this complex yields the formally iridium(IV) dimer  $[(C_5(CH_3)_5)IrH_3]_2$ . Use of the more nucleophilic reducing agent  $LiEt_3BH$  in this reaction leads to the mononuclear salt  $(C_5(CH_3)_5)IrH_3[Li(THF)_x]$  (**5**), the anion of which may be hydrolyzed to the iridium(V) complex  $(C_5(CH_3)_5)IrH_4$  (**6**). The overall mechanism of the formation of tetrahydride **6** is discussed on the basis of these results. Deprotonation of **6** with *t*-BuLi in the presence of pmdeTA leads to the sequestered salt  $(C_5(CH_3)_5)IrH_3[Li(pmdeTA)]$  (**8**). Silyl- or stannylated of the anion occurs with  $Me_3SiO_3SCF_3$ ,  $Me_3SnCl$ , and  $Ph_3SnBr$  to yield the new iridium(V) polyhydrides  $(C_5(CH_3)_5)IrH_3SiMe_3$ ,  $(C_5(CH_3)_5)IrH_3SnMe_3$ , and  $(C_5(CH_3)_5)IrH_3SnPh_3$ , the last of which was structurally characterized by a single-crystal X-ray diffraction study.

The hydride ligand is important in organometallic chemistry: metal hydrides are implicated in various homogeneous and heterogeneous catalytic processes,<sup>1</sup> and polyhydride complexes are known to be active catalysts for H/D exchange.<sup>2</sup> From a structural standpoint, the small van der Waals volume of hydrogen atoms and the ability of hydride ligands to move from bridging to terminal sites (similar to CO) make polyhydride complexes worthy of study;<sup>3</sup> the difficulty inherent in determining hydride positions by NMR or X-ray study presents a fascinating challenge. Of greatest interest to us is the well-documented ability of hydride ligands to stabilize the higher formal oxidation states of transition metals;<sup>4</sup> no other ligand forms as many high-oxidation-state complexes as the hydrogen atom.

In general, little is known of the mechanism of preparing organometallic hydride species from organometallic halides and hydridic reducing agents, in spite of the fact that no method is more commonly used.<sup>3c,d</sup> In addition, one aspect of this chemistry is the well-documented result that oxidation of the metal center often occurs,<sup>3c,d</sup> even though the medium should be considered reducing. Studies have not yet definitively established the mechanisms of such oxidations.<sup>5</sup>

In 1983, we reported the synthesis of  $(C_5(CH_3)_5)IrH_4$ ,<sup>6a</sup> one of the few organometallic iridium(V) complexes,<sup>6b</sup> starting with the iridium(III) dimer  $[(C_5(CH_3)_5)Ir]_2(\mu-H)_3PF_6$  and the reducing agent  $LiEt_3BH$ . In addition to the question of the source of each iridium-bound hydrogen, we were perplexed by the formal oxidation of the iridium atoms in what one presumed would be a reducing medium. The high yields of tetrahydride demonstrated that one possibility, oxidation of half the iridium and reduction

of the other half, did not obtain.

In order to study the mechanism of the formation of  $(C_5(CH_3)_5)IrH_4$ , we drew upon our data for (trimethylphosphine)-(pentamethylcyclopentadienyl)iridium polyhydrides<sup>7</sup> and undertook to synthesize potential intermediates in the transformation. In addition, we attempted to expand the range of iridium(V) complexes known in order to increase the data for high-oxidation-state species. Our results are described in this paper.

## Experimental Section

**General.** Experimental conditions were described in the previous paper.<sup>7</sup> <sup>1</sup>H, <sup>11</sup>B, and <sup>13</sup>C NMR spectra were recorded on the 180, 200, 250, 300, and 500 MHz instruments at the UCB NMR facility and are reported as ppm downfield of  $Me_4Si$  (<sup>1</sup>H, <sup>13</sup>C) or saturated  $NaBF_4$  in methanol (<sup>11</sup>B).

$[(C_5(CH_3)_5)Ir]_2H_3BH_4$  (**2**). A slurry of  $LiBH_4$  (77 mg, 3.55 mmol) and  $[(C_5(CH_3)_5)Ir]_2(\mu-H)_3PF_6$ <sup>7,8a</sup> (**1**-PF<sub>6</sub>, 408 mg, 0.508 mmol) in 10% THF/pentane (both freshly distilled) was stirred for 3 h at ambient temperature. Removal of the solvent in vacuo without heating yielded an orange-yellow solid, which was extracted with pentane (3 × 15 mL). The extracts were filtered through Celite packed in a frit, whereupon approximately half the pentane was evaporated. Upon cooling the solution to -40 °C, bright yellow-orange material crystallized and was collected by filtration and washed with cold pentane. Successive evaporations and crystallizations of the mother liquor gave two additional crops of product indistinguishable from the first by <sup>1</sup>H NMR, for a total yield of 216 mg (63%) of **2**. The compound is quite thermally sensitive; solutions of **2** decompose at 60 °C within 5 min and at 23 °C over 48 h. <sup>1</sup>H NMR ( $C_6D_6$ )  $\delta$  1.92 (s, 30 H,  $C_5Me_5$ ); -14.18 (br, 2 H, Ir-H<sub>bridge</sub>-B); -17.51 (s, 1 H, Ir-H<sub>bridge</sub>-Ir); -17.78 (s, 2 H, Ir-H<sub>1</sub>). <sup>1</sup>H{<sup>11</sup>B} NMR (toluene-*d*<sub>8</sub>, -50 °C)  $\delta$  5.52 (br, 2 H, BH<sub>2</sub>); 1.91 (s, 30 H,  $C_5Me_5$ ); -14.10 (br, 2 H, Ir-H<sub>bridge</sub>-B); -17.46 (s, 1 H, Ir-H<sub>bridge</sub>-Ir); -17.69 (s, 2 H, Ir-H<sub>1</sub>). <sup>11</sup>B{<sup>1</sup>H} NMR (toluene-*d*<sub>8</sub>, -50 °C)  $\delta$  5.5 (br s). <sup>13</sup>C{<sup>1</sup>H} NMR ( $C_6D_6$ )  $\delta$  94.1 (s,  $C_5Me_5$ ); 10.5 (s,  $C_5Me_5$ ). IR (KBr)  $\nu$  2430, 2360, 2290 (all s, B-H); 2115 (s, Ir-H<sub>1</sub>), 2040 (sh), 1155 (s, Ir-H<sub>bridge</sub>)  $cm^{-1}$ . EIMS (20 eV, 23 °C), *m/e* 672, 671, 670, 669, 668, 667. Anal. Calcd for  $C_{20}H_{37}Ir_2B$ : C, 35.71; H, 5.54. Found: C, 35.88; H, 5.66.

$[(C_5(CH_3)_5)IrH_3]_2$  (**3**). Trihydride dimer **1**-PF<sub>6</sub> (401 mg, 0.500 mmol) and  $LiBH_4$  (65.3 mg, 3.00 mmol) were slurried in 2% THF in hexane (50 mL). After the mixture was stirred overnight, the homogeneous solution containing **2** was filtered through hexane-wetted alumina III packed in a frit, after which the alumina was washed with benzene to give

(7) Gilbert, T. M.; Bergman, R. G. *J. Am. Chem. Soc.*, preceding paper in this issue.

(8) (a) White, C.; Oliver, A. J.; Maitlis, P. M. *J. Chem. Soc., Dalton Trans.* 1973, 1901. (b) Gill, D. S.; Maitlis, P. M. *J. Organomet. Chem.* 1975, 87, 359.

(1) Muetterties, E. L., Ed. "Transition Metal Hydrides"; New York: Marcel Dekker, 1971.

(2) Parshall, G. W. *Acc. Chem. Res.* 1975, 8, 113.

(3) For recent reviews, see: (a) Bau, R., Ed. "Transition Metal Hydrides"; Marcel Dekker: New York, 1978, Adv. Chem. Ser. No. 167. (b) Teller, R. G.; Bau, R. *Struc. Bonding (Berlin)* 1981, 44, 1. (c) Soloveichik, G. L.; Bulychev, B. M. *Russ. Chem. Rev.* 1982, 51, 286. (d) Moore, D. S.; Robinson, S. D. *Chem. Soc. Rev.* 1983, 12, 415.

(4) Reference to high oxidation states is meant in a formal electron-counting sense when applied to organometallic polyhydride species; a deficiency of electron density at the metal center is not necessarily implied. See: Crabtree, R. H. *Acc. Chem. Res.* 1979, 12, 331.

(5) Labinger, J. A.; Wong, K. S. *J. Organomet. Chem.* 1979, 170, 373.

(6) (a) Gilbert, T. M.; Bergman, R. G. *Organometallics* 1983, 2, 1458. (b) Isobe, K.; Vasquez de Miguel, A.; Nutton, A.; Maitlis, P. M. *J. Chem. Soc., Dalton Trans.* 1984, 929 and references therein.

an orange solution. The solutions were combined, the solvent removed, and the residue recrystallized from pentane to give deep orange-burgundy crystals (116 mg, 35%). A somewhat impure second crop could be obtained.  $^1H$  NMR ( $C_6D_6$ , room temperature)  $\delta$  1.97 (s, 30 H,  $C_5Me_5$ ); -14.76 (s, 6 H, Ir-H).  $^1H$  NMR (3:2 THF- $d_6$ /toluene- $d_8$ , -120 °C)  $\delta$  1.94 (s, 30 H,  $C_5Me_5$ ); -10.70 (br s, 2 H, Ir-H<sub>bridg</sub>); -17.11 (br s, 4 H, Ir-H<sub>1</sub>).  $^{13}C\{^1H\}$  NMR ( $C_6D_6$ )  $\delta$  93.0 (s,  $C_5Me_5$ ); 10.2 (s,  $C_5Me_5$ ). IR ( $C_6H_6$ )  $\nu_{Ir-H}$  2100; IR (KBr) 2120 (terminal hydride), 1190, 1120 (both br, bridging hydride)  $cm^{-1}$ . EIMS (15 eV, room temperature),  $m/e$  659, 658, 657, 656, 654. Anal. Calcd for  $C_{20}H_{36}Ir_2$ : C, 36.35; H, 5.49. Found: C, 36.30; H, 5.32. Solid-state decomposition temperature 60–80 °C.

In a separate experiment, the reaction mixture was hydrolyzed through the addition of methanol (125 mmol) at 0 °C, giving a yellow-orange solution. After evaporation of solvent, the resulting residue was extracted with toluene (12 mL). The filtered extracts were layered with hexane and cooled to -40 °C, ultimately yielding orange crystals of **3** identical by  $^1H$  NMR with those from the procedure above (128 mg, 38%).

**Reaction of 3 with  $P(CH_3)_3$ .**  $P(CH_3)_3$  (0.200 mmol) was vacuum transferred into a  $C_6D_6$  solution of **3** (33.2 mg, 0.050 mmol) in an NMR tube. The yellow solution was warmed to 55 °C for 6 h, at which point no color remained. Inspection of the  $^1H$  NMR demonstrated clean conversion of starting material to  $(C_5(CH_3)_5)Ir(P(CH_3)_3)_2H_2$  (0.073 mmol by integration against internal  $(Me_3Si)_2O$ , 73%).

**Generation and Reactions of  $(C_5(CH_3)_5)IrH_3[Li(THF)_x]$  (**5**).**  $LiEt_3BH$  (1.0 mmol) with added dropwise to a slurry of **1-PF<sub>6</sub>** (240 mg, 0.299 mmol) in 1:1 toluene/hexane (6 mL). After being stirred for 3 h, the homogeneous solution was cooled to -40 °C. Deep red-orange crystals precipitated; these were filtered, washed with hexane, and dried to yield 215 mg of material. At this point,  $^1H$  NMR showed a great deal of THF and  $BEt_3/BEt_3H^-$  present in the product. High vacuum could not completely remove the solvent; it was noted that the solubility of the material decreased dramatically as the THF was removed (see compound **7** below). As discussed in the text, spectral and chemical evidence strongly suggests that this material is  $(C_5(CH_3)_5)IrH_3[Li(THF)_x]$ , by analogy with **8**.  $^1H$  NMR ( $C_6D_6$ )  $\delta$  2.18 (br s, 15H,  $C_5Me_5$ ); -19.22 (br s, 3 H, Ir-H); 3.55, 1.40 (THF); 1.45, 1.27 ( $BEt_3/BEt_3H^-$ ).  $^{13}C\{^1H\}$  NMR ( $C_6D_6$ )  $\delta$  87.4 (s,  $C_5Me_5$ ); 11.3 (s,  $C_5Me_5$ ); 67.3, 24.4 (THF); 16.0, 11.0 ( $BEt_3/BEt_3H^-$ ). IR ( $C_6H_6$ )  $\nu_{Ir-H}$  2019 (br)  $cm^{-1}$ .

In a second experiment designed to characterize **5** chemically, a hexane slurry of **1-BF<sub>4</sub>** (186 mg, 0.250 mmol) and pmdeta (433 mg, 2.5 mmol) was treated dropwise with  $LiEt_3BH$  (1.5 mmol) from which most of the THF had been evaporated and replaced with toluene. The solution slowly became homogeneous during 20 h of stirring. The solvent was removed in vacuo, and the oily residue was extracted with hexane followed by benzene. The solvent was removed from the filtered extracts and the burgundy residue dissolved in hexane. Cooling to -40 °C gave 26 mg of an unidentified  $BEt_3$ /pmdeta adduct as shown by  $^1H$  NMR. Filtration and refrigeration of the mother liquor gave two crops of  $(C_5(CH_3)_5)IrH_3[Li(pmdeta)]$  (**8**) shown to be >85% pure by  $^1H$  NMR (70 mg, 0.137 mmol, 27%). The  $BEt_3/BEt_3H^-$ -containing impurity could not be removed by crystallization.

In a third experiment, a  $^1H$  NMR sample of **5** was treated with methanol (50  $\mu$ L). The orange solution decolorized as black solid precipitated. Inspection of the  $^1H$  NMR of the sample demonstrated the presence of THF and only one organometallic product,  $(C_5(CH_3)_5)IrH_4$  (**6**).

Finally, adding **5** (70 mg) in 1:1 toluene/hexane to a hexane slurry of  $Ph_3SnBr$  (35 mg, 0.081 mmol) at -78 °C, stirring for 2 h at this temperature, warming to room temperature, and evaporating the solvent gave a brown-white semisolid. Recrystallization from ether/pentane gave two crops of colorless crystals of **9c** (30 mg, 0.0441 mmol, 18% based on **1-PF<sub>6</sub>**), shown to be pure by  $^1H$  NMR.

**$(C_5(CH_3)_5)IrH_4$  (**6**).** A slurry of **1-PF<sub>6</sub>** (2.01 g, 2.50 mmol) in hexane (200 mL) was cooled to -40 °C and then treated dropwise with  $LiEt_3BH$  (15 mmol) from which most of the THF had been removed and replaced with an equivalent volume of toluene. Overnight stirring at room temperature resulted in a deep orange, homogeneous solution which was cooled to -40 °C and then filtered through hexane-wetted alumina III packed in a frit. The alumina was washed with benzene to give a pale yellow solution. Removal of the solvent from the combined solutions and two sublimations of the yellow-white residue (30–40 °C, 100 mtorr) gave 1.23 g (74%) of pure white crystals. The crystal structure of this compound has been reported.<sup>6a</sup>  $^1H$  NMR ( $C_6D_6$ )  $\delta$  1.99 (s, 15 H,  $C_5Me_5$ ); -15.43 (s, 4 H, Ir-H).  $^{13}C\{^1H\}$  NMR ( $C_6D_6$ )  $\delta$  96.5 (s,  $C_5Me_5$ ); 10.0 (s,  $C_5Me_5$ ). IR (KBr)  $\nu_{Ir-H}$  2150  $cm^{-1}$ . UV ( $C_6H_{12}$ )  $\lambda_{max}$  215 nm ( $\epsilon =$

5000). Anal. Calcd for  $C_{10}H_{19}Ir$ : C, 36.24; H, 5.78. Found: C, 35.98; H, 5.83. Solid-state decomposition temperature 50–100 °C.

**$(C_5(CH_3)_5)IrH_3Li$  (**7**).** A pentane solution of tetrahydride **6** (410 mg, 1.24 mmol) was treated dropwise with *t*-BuLi (1.50 mmol). White solid precipitated instantly from the solution. After the solution was stirred for 30 min, the powdery material was filtered and washed with pentane to give 371 mg (89%) of slightly pyrophoric material. Methanol hydrolysis of this material in an NMR tube reaction instantly generated **6** as the only product by  $^1H$  NMR.

The total insolubility of the compound in inert solvents precluded most spectral characterizations. IR (KBr)  $\nu_{Ir-H}$  2060 (br)  $cm^{-1}$ . Anal. Calcd for  $C_{10}H_{18}IrLi$ : C, 35.60; H, 5.38. Found: C, 35.98; H, 5.62.

**$(C_5(CH_3)_5)IrH_3[Li(pmdeta)]$  (**8**).** At -78 °C (dry ice/acetone), a pentane solution of **6** (680 mg, 2.05 mmol) and pmdeta (1.40 mL, 8.08 mmol) was treated dropwise over 15 min with *t*-BuLi (3.40 mmol) in 10 mL of pentane. After the solution was stirred for 1.5 h at this temperature, the pale yellow-white solid was filtered and dried to give highly air-sensitive **8** (295 mg, 28%).  $^1H$  NMR ( $C_6D_6$ )  $\delta$  2.52 (br s, 15 H,  $C_5Me_5$ ); 2.16 (s, 3 H, internal amine -CH<sub>3</sub>); 2.05 (s, 12 H, terminal amine -CH<sub>3</sub>); -19.21 (br s, 3 H, Ir-H).  $^{13}C\{^1H\}$  NMR ( $C_6D_6$ )  $\delta$  85.0 (s,  $C_5Me_5$ ); 56.1, 52.9 (s, amine methylenes); 45.9 (s, terminal amine -CH<sub>3</sub>); 45.1 (s, internal amine -CH<sub>3</sub>); 12.2 (s,  $C_5Me_5$ ). IR ( $C_6H_6$ )  $\nu_{Ir-H}$  2020 (br)  $cm^{-1}$ . Signer<sup>10</sup> molecular weight ( $C_6H_6$ , 25 °C, slight decomposition noted during equilibration) calcd 511, found 445. Anal. Calcd for  $C_{19}H_{41}N_3IrLi$ : C, 44.68; H, 8.09; N, 8.23. Found: C, 44.31; H, 8.27; N, 8.16.

A sample of **8** (15.0 mg, 0.0294 mmol) slurried in pentane was treated with isopropyl alcohol (250  $\mu$ L). After the mixture was stirred for 5 min, the solvent was evaporated and the residue taken into  $C_6D_6$ . Inspection of the  $^1H$  NMR demonstrated free pmdeta and **6** (0.0250 mmol by integration vs. internal  $(Me_3Si)_2O$ , 85%) to be the only  $^1H$  NMR active species present in the solvent.

**$(C_5(CH_3)_5)IrH_3(SiMe_3)$  (**9a**).** A toluene solution of **8** (51 mg, 0.100 mmol) was added dropwise to a pentane solution of  $Me_3SiO_3SCF_3$  (26.7 mg, 0.120 mmol) at -78 °C. The pale yellow solution was stirred for 5 h and then allowed to warm slowly to room temperature. Following removal of solvent, the residue was dissolved in benzene and filtered through Celite to remove insoluble material and the benzene evaporated to yield a yellow-white solid. Sublimation (5 mtorr, 45 °C) gave pure white product (31 mg, 0.077 mmol, 76%).  $^1H$  NMR (toluene- $d_8$ , room temperature)  $\delta$  1.91 (s, 15 H,  $C_5Me_5$ ); 0.61 (s, 9 H,  $SiMe_3$ ); -16.20 (s, 3 H, Ir-H).  $^1H$  NMR (toluene- $d_8$ , -80 °C)  $\delta$  1.79 (s, 15 H,  $C_5Me_5$ ); 0.80 (s, 9 H,  $SiMe_3$ ); -15.83 (t,  $J_{HH} = 5.6$  Hz, 1 H, Ir-H<sub>1</sub>); -16.00 (d,  $J_{HH} = 5.6$  Hz, 2 H, Ir-H<sub>cis</sub>).  $^{13}C\{^1H\}$  NMR (toluene- $d_8$ )  $\delta$  96.9 (s,  $C_5Me_5$ ); 10.6 (s,  $C_5Me_5$ ); 9.95 (s,  $SiMe_3$ ). IR (KBr)  $\nu_{Ir-H}$  2195, 2160  $cm^{-1}$ . EIMS (13 eV, room temperature),  $m/e$  404, 402. Anal. Calcd for  $C_{13}H_{27}IrSi$ : C, 38.68; H, 6.74. Found: C, 38.39; H, 6.57. Solid-state decomposition temperature 110–120 °C.

**$(C_5(CH_3)_5)IrH_3(SnMe_3)$  (**9b**).** A toluene solution of **8** (51 mg, 0.100 mmol) was added dropwise to a pentane solution of  $Me_3SnCl$  (30 mg, 0.150 mmol) at 0 °C. After the mixture was stirred for 4 h at this temperature, the solvent was removed and the resulting oil taken up in pentane. The pentane solution was filtered through Celite and the solvent evaporated. Sublimation of the resultant oily residue (30 mtorr, 30 °C, LN<sub>2</sub>-cooled cold finger) gave greasy white crystals of **9b** (16 mg, 33%).  $^1H$  NMR (toluene- $d_8$ , room temperature)  $\delta$  1.94 (s,  $J_{Sn-H} < 1$  Hz, 15 H,  $C_5Me_5$ ); 0.50 ( $J_{Sn-H} = 47.8$  Hz, 9 H,  $SnMe_3$ ); -16.32 ( $J_{Sn-H} = 23.6$  Hz, 3 H, Ir-H).  $^1H$  NMR (toluene- $d_8$ , -80 °C)  $\delta$  1.81 (s,  $J_{Sn-H} < 1$  Hz, 15 H,  $C_5Me_5$ ); 0.68 ( $J_{Sn-H} = 48.0$  Hz, 9 H,  $SnMe_3$ ); -15.87 (t,  $J_{HH} = 6.5$  Hz, 1 H, Ir-H<sub>1</sub>); -16.15 (d,  $J_{HH} = 6.5$  Hz, 2 H, Ir-H<sub>cis</sub>).  $^{13}C\{^1H\}$  NMR (toluene- $d_8$ )  $\delta$  95.8 (s,  $C_5Me_5$ ); 10.9 (s,  $C_5Me_5$ ); -5.0 (br s,  $SnMe_3$ ). IR (thin film)  $\nu_{Ir-H}$  2160 (sh), 2120 (s)  $cm^{-1}$ . EIMS (70 eV, room temperature), envelopes centered around  $m/e$  479, 461, 443. Anal. Calcd for  $C_{13}H_{27}IrSn$ : C, 31.59; H, 5.51. Found: C, 31.80; H, 5.36.

**$(C_5(CH_3)_5)IrH_3(SnPh_3)$  (**9c**).** A toluene slurry of anion **7** (84.4 mg, 0.250 mmol) was treated dropwise with  $Ph_3SnBr$  (139.5 mg, 0.324 mmol) dissolved in toluene. After the solution was stirred for 5 days, filtration of the solution, removal of the solvent, and recrystallization from ether/hexane gave white crystals (112 mg, 66%) of product. The crystal used in the X-ray diffraction study crystallized from a saturated pentane solution.  $^1H$  NMR (toluene- $d_8$ , 80 °C)  $\delta$  7.8–7.1 (complex, 15 H,  $SnPh_3$ ); 1.84 (br s,  $J_{SnH} < 1$  Hz, 15 H,  $C_5Me_5$ ); -15.69 ( $J_{SnH} = 28.2$  Hz, 3 H, Ir-H).  $^1H$  NMR (toluene- $d_8$ , -65 °C)  $\delta$  7.9–7.1 (complex, 15 H,  $SnPh_3$ ); 1.70 (br s,  $J_{SnH} < 1$  Hz, 15 H,  $C_5Me_5$ ); -15.36 (d,  $J_{HH} = 8.1$  Hz, 2 H, Ir-H<sub>cis</sub>); -15.58 (t,  $J_{HH} = 8.1$  Hz, 1 H, Ir-H<sub>1</sub>).  $^{13}C\{^1H\}$  NMR (acetone- $d_6$ )  $\delta$  144.1 (s, Ph); 137.4 ( $J_{SnC} = 37.8$  Hz, Ph); 128.5 (overlapping, Ph); 97.7 (s,  $C_5Me_5$ ); 10.8 (s,  $C_5Me_5$ ). IR (KBr)  $\nu_{Ir-H}$  2190, 2105  $cm^{-1}$ . EIMS,  $m/e$  680, 600, 524, 442. Mp 150–160 °C dec. Anal.

(9) (a) Janowicz, A. H.; Bergman, R. G. *J. Am. Chem. Soc.* **1982**, *104*, 351. (b) Janowicz, A. H.; Bergman, R. G. *J. Am. Chem. Soc.* **1983**, *105*, 3929.

(10) Clark, E. P. *Ind. Eng. Chem., Anal. Ed.* **1941**, *13*, 820.

Table I. Cell Constants and Data Collection Parameters for the X-ray Diffraction Experiments

	$2 \cdot \frac{1}{3} \text{C}_5\text{H}_{12}$ ( $-90^\circ \text{C}$ )	$9c$ ( $25^\circ \text{C}$ )
(A) Crystal Parameters		
$a$ , Å	15,466 (3) <sup>a</sup>	9,7438 (9) <sup>b</sup>
$b$ , Å		11,1893 (10)
$c$ , Å		11,1364 (12)
$\alpha$ , deg	81.941 (12)	101,382 (6)
$\beta$ , deg		98.282 (9)
$\gamma$ , deg		94.786 (8)
$V$ , Å <sup>3</sup>	3599 (2)	1275.1 (4)
space group	$R\bar{3}c$	$P\bar{1}$
$Z$	6	2
$d_{\text{calcd}}$ , g/cm <sup>3</sup>	1.86	1.77
$\mu_{\text{calcd}}$ , cm <sup>-1</sup>	110.4	61.89
size, mm	$0.25 \times 0.28 \times 0.30$	$0.18 \times 0.23 \times 0.25$
(B) Data Measurement Parameters		
radiation	Mo K $\alpha$ ( $\lambda = 0.71073$ Å)	
monochromator	highly oriented graphite ( $2\theta = 12.2^\circ$ )	
detector	crystal scintillation counter, with PHA	
reflcs measd	$+h, +k, \pm l$ (in hexagonal cell)	$+h, \pm k, \pm l$
$2\theta$ range, deg	3–45	3–55
scan type	$\theta$ – $2\theta$	$\theta$ – $2\theta$
scan speed	$0.8 \rightarrow 6.7$ ( $\theta$ , deg/min)	$1.2 \rightarrow 6.7$ ( $\theta$ , deg/min)
scan width	$\Delta\theta = 0.7 + 0.347 \tan \theta$	$\Delta\theta = 0.5 + 0.347 \tan \theta$
background	0.25 ( $\Delta\theta$ ) at each end	0.25 ( $\Delta\theta$ ) at each end
aperture $\rightarrow$ crystal, mm	173	173
vertical aperture, mm	3.0	3.0
horizontal aperture, mm	$2.5 + 1.0 \tan \theta$ (var)	$2.0 + 1.0 \tan \theta$ (var)
reflcs collected	3528	6630
unique reflcs	1570	5857

<sup>a</sup> Unit cell parameters and their esds were derived by a least-squares fit to the setting angles of the unresolved Mo K $\alpha$  components of 24 reflections with  $2\theta$  near  $28^\circ$ . <sup>b</sup> Unit cell parameters and their esds were derived by a least-squares fit to the setting angles of the unresolved Mo K $\alpha$  components of 24 reflections with  $2\theta$  between  $25^\circ$  and  $32^\circ$ .

Calcd for  $\text{C}_{28}\text{H}_{33}\text{IrSn}$ : C, 49.42; H, 4.89. Found: C, 49.96; H, 5.09. Repeated crystallization did not result in improved analyses.

This compound was also prepared from the pmdda-sequestered lithium salt **8** at  $-78^\circ \text{C}$  in 88% recrystallized yield, shown to be pure by <sup>1</sup>H NMR.

**Single-Crystal X-ray Diffraction Study of  $2 \cdot \frac{1}{3} \text{C}_5\text{H}_{12}$ .** Single crystals of **2** suitable for diffraction study were grown from cold pentane solution as partial pentane solvates. Elemental analysis for boron with these crystals gave acceptable values. Assuming a stoichiometry of  $[(\text{C}_5(\text{CH}_3)_5)\text{Ir}]_2\text{H}_3\text{BH}_4 \cdot \frac{1}{3} \text{C}_5\text{H}_{12}$ , anal. calcd for  $\text{C}_{21.67}\text{H}_{41}\text{Ir}_2\text{B}$ : B, 1.55. Found: B, 1.5.

A cleaved single crystal of  $2 \cdot \frac{1}{3} \text{C}_5\text{H}_{12}$  was mounted on a glass fiber and then coated with polycyanoacrylate cement. The crystal was mounted on the UCB CHEXRAY Enraf-Nonius CAD-4 diffractometer,<sup>11</sup> centered in the beam and cooled to  $-90 \pm 3^\circ \text{C}$  by a stream of cold nitrogen gas. Automatic peak search and indexing procedures yielded a rhombohedral reduced primitive cell with systematic absences consistent with the space group  $R\bar{3}c$  or  $R\bar{3}c$ . Final cell parameters and specific data collection parameters are given in Table I. Three intensity standards were checked every 2 h of X-ray exposure time. Three orientation standards were checked every 250 reflections, and the crystal orientation was redetermined if any of the reflections were offset more than  $0.1^\circ$  from their predicted positions; reorientation was needed twice during data collection.

The 3258 raw intensity data were converted to structure factor amplitudes and their esds by correction for scan speed, background, and Lorentz and polarization effects. Inspection of the intensity standards showed a monotonic isotropic decrease to 0.92 of the original intensity; the data were corrected for this decay. Inspection of azimuthal scan data<sup>12</sup> showed a variation of  $I_{\text{min}}/I_{\text{max}} = 0.77$  for the average curve; an

empirical absorption correction based on these data was applied to the intensities. Removal of systematically absent and averaging of redundant data ( $R(I) = 3.1\%$ ) left 1570 unique data.

The structure was solved by Patterson methods and refined via standard least-squares and Fourier techniques. The assumption that the space group was  $R\bar{3}c$  was confirmed by the successful solution and refinement of the structure. In a difference Fourier map calculated following refinement of all non-hydrogen atoms with anisotropic thermal parameters, peaks corresponding to the expected positions of most of the hydrogen atoms were found. In addition a set of moderately large peaks was found near the position of 32 symmetry at  $(\frac{1}{4}, \frac{1}{4}, \frac{1}{4})$ . These peaks were assumed to be due to a highly disordered partial molecule of pentane. Three positions (CP(11), CP(12), CP(13)) were refined with carbon scattering factors, isotropic thermal parameters, and occupancies constrained to represent equivalent amounts of electron density for each site. The refinement of the occupancy converged well to a value of 0.50 for the carbons in general positions (CP(12) and CP(13)), and 0.167 for the carbon located on a crystallographic threefold axis (CP(11)). Adding the occupancies and summing to calculate electron density gives approximately 42 electrons per site. Pentane,  $\text{C}_5\text{H}_{12}$ , has 42 electrons per molecule, including the hydrogen atoms. Thus the results of the refinement are consistent with one disordered pentane molecule occupying each site, giving a stoichiometric ratio of one molecule of pentane for every three iridium dimers, or equally, one-third molecule of pentane per iridium dimer.

The hydrogen atoms on the pentamethylcyclopentadiene ligand were fixed during the first cycles of refinement, but they were later allowed to refine. The terminal hydrogen atoms attached to the iridium (H(1) and H(2)) were immediately obvious in difference Fourier maps and refined well. The bridging hydrogen (H(3)) and the boron-bound hydrogen (H(4)) were less obvious, so various models were tried before settling on the final one. Obvious correlation existed between the placement of atoms on the crystallographic twofold axis and the refinement of the "pentane" atoms.

In the final cycles of refinement the (222) and (021) reflections were removed from the data set as being adversely affected by extinction. There was no other evidence of effects of extinction. Inspection of the final residuals ordered in ranges of  $\sin \theta/\lambda$ ,  $F_{\text{obsd}}$  parity, and  $hkl$  values showed no unusual features.

The quantity minimized by the least-squares program was  $\sum w(F_o - F_c)^2$ , where  $w$  is the weight of a given reflection. The  $p$  factor, used to reduce the weight of intense reflections, was set to 0.02 throughout the refinement. The analytical forms of the scattering factor tables for the neutral atoms were used, and all non-hydrogen scattering factors were corrected for both the real and imaginary components of anomalous dispersion.

The largest peak in the final difference Fourier map had an electron density of  $0.86 \text{ e}/\text{\AA}^3$ . All peaks larger than  $0.5 \text{ e}/\text{\AA}^3$  were located near iridium atoms except peak 2, near H(3).

The final residuals for 190 variables refined against the 1143 data for which  $F^2 > 3\sigma F^2$  were  $R = 2.00\%$ ,  $R_w = 2.08\%$ ,  $R_{\text{all}} = 3.89\%$ , with GOF = 0.897.

Positional and thermal parameters for the refined atoms are given in Table II. A listing of  $F_o$  and  $F_c$  is available as Supplementary Material.

**Single-Crystal X-ray Diffraction Study of  $9c$ .** Two colorless single crystals of **9c** grown from pentane were mounted on glass fibers with polycyanoacrylate cement. Preliminary study and alignment on the diffractometer closely paralleled the procedures for **2**. The first data crystal was placed on the diffractometer and automatic peak search and indexing procedures used to yield a triclinic reduced primitive cell. Data collection proceeded for the hemisphere  $h < 0$ ; significant decay was noted in the intensity standards as the cell dimensions gradually changed. After collection of the first hemisphere, the second crystal was placed on the diffractometer and collection proceeded for the hemisphere  $h > 0$ . The structure was solved by using the data from the first crystal, but the iridium-bound hydrogen atoms could not be located with those data. The structure as reported is based on data from the second crystal only, and the final cell parameters and data collection parameters given in Table I are for that crystal. Intensity and orientation standards were checked as noted above; reorientation was needed twice during data collection for the second crystal.

The raw intensity data were converted to structure factor amplitudes as for **2**. Inspection of the intensity standards showed a monotonic, slightly anisotropic decay to 0.70 of the original intensity (second crystal); the data were corrected for this decay. An absorption correction based

(11) The instrumentation, methods of data collection, computer programs, and formulae for data reduction and structure solution have been described: Theopold, K. H.; Bergman, R. G. *J. Am. Chem. Soc.* **1983**, *105*, 464.

(12) Reflections used for azimuthal scans were located near  $\chi = 90^\circ$ , and the intensities were measured at  $10^\circ$  increments of rotation of the crystal about the diffraction vector.

**Table II.** Positional Parameters and Their Estimated Standard Deviations for  $2 \cdot 1/3 C_5H_{12}^b$ 

atom	x	y	z	$B, \text{\AA}^2$
Ir(1)	0.11771 (2)	0.44681 (2)	0.66326 (1)	3.192 (5)
C(1)	0.1798 (4)	0.5147 (4)	0.5442 (4)	4.2 (2)
C(2)	0.2437 (4)	0.4944 (4)	0.6032 (4)	4.1 (2)
C(3)	0.2148 (4)	0.5391 (4)	0.6765 (4)	3.4 (1)
C(4)	0.1327 (4)	0.5897 (4)	0.6631 (4)	3.7 (2)
C(5)	0.1116 (4)	0.5764 (4)	0.5793 (5)	4.4 (2)
C(6)	0.1865 (6)	0.4918 (5)	0.4530 (5)	8.0 (2)
C(7)	0.3299 (5)	0.4369 (5)	0.5871 (6)	6.8 (2)
C(8)	0.2651 (5)	0.5373 (5)	0.7530 (5)	6.0 (2)
C(9)	0.0810 (5)	0.6502 (5)	0.7229 (6)	7.1 (2)
C(10)	0.0370 (5)	0.6250 (5)	0.5364 (6)	8.4 (2)
CP(11)	0.319 (2)	0.319	0.319	17 (2) <sup>a</sup>
CP(12)	0.240 (2)	0.286 (2)	0.342 (2)	17 (1) <sup>a</sup>
CP(13)	0.213 (3)	0.194 (2)	0.319 (2)	21 (1) <sup>a</sup>
B(1)	0.1695 (6)	0.330	0.750	5.0 (2)
H(1)	0.048 (4)	0.409 (4)	0.630 (4)	6 (2) <sup>a</sup>
H(2)	0.133 (4)	0.346 (4)	0.645 (4)	7 (2) <sup>a</sup>
H(3)	0.050 (7)	0.450	0.750	17 (5) <sup>a</sup>
H(4)	0.158 (4)	0.260 (4)	0.737 (4)	6 (2) <sup>a</sup>
H(61)	0.219 (4)	0.526 (4)	0.410 (4)	6 (2) <sup>a</sup>
H(62)	0.214 (5)	0.442 (5)	0.458 (5)	9 (2) <sup>a</sup>
H(63)	0.145 (4)	0.471 (4)	0.432 (4)	6 (2) <sup>a</sup>
H(71)	0.373 (3)	0.465 (3)	0.551 (3)	5 (1) <sup>a</sup>
H(72)	0.364 (8)	0.443 (7)	0.642 (8)	22 (5) <sup>a</sup>
H(73)	0.325 (4)	0.396 (4)	0.555 (4)	7 (2) <sup>a</sup>
H(81)	0.293 (3)	0.588 (3)	0.743 (3)	4 (1) <sup>a</sup>
H(82)	0.234 (5)	0.543 (5)	0.800 (5)	9 (2) <sup>a</sup>
H(83)	0.306 (5)	0.466 (4)	0.769 (5)	9 (2) <sup>a</sup>
H(91)	0.098 (4)	0.698 (4)	0.712 (4)	8 (2) <sup>a</sup>
H(92)	-0.000 (4)	0.669 (5)	0.716 (5)	10 (2) <sup>a</sup>
H(93)	0.079 (5)	0.631 (5)	0.768 (5)	9 (2) <sup>a</sup>
H(101)	0.042 (4)	0.695 (4)	0.526 (4)	7 (2) <sup>a</sup>
H(102)	0.029 (4)	0.595 (4)	0.496 (4)	6 (2) <sup>a</sup>
H(103)	0.001 (4)	0.626 (4)	0.552 (4)	5 (2) <sup>a</sup>

<sup>a</sup> Atoms refined with isotropic thermal parameters. <sup>b</sup> Anisotropically refined atoms are given in the form of the isotropic equivalent thermal parameter defined as  $(4/3)[a^2B(1,1) + b^2B(2,2) + c^2B(3,3) + ab(\cos \gamma)B(1,2) + ac(\cos \beta)B(1,3) + bc(\cos \alpha)B(2,3)]$ .

on the measured shape and size of the crystal and an  $8 \times 8 \times 10$  Gaussian grid of internal points was applied to the data after solution of the structure confirmed the unit cell contents ( $T_{\max} = 0.396$ ,  $T_{\min} = 0.301$ ). Removal of a series of badly measured data which had been remeasured left 5857 unique data.

The structure was solved by Patterson methods. The assumption that the space group was  $P\bar{1}$  was confirmed by successful solution and refinement. Refinement of the data on the first crystal led to the location of the hydrogen atoms on the organic ligands but not the iridium-bound hydrogen atoms.

At this point the data set from the second crystal was reduced and refinement continued with use of those data. In a difference Fourier map calculated following refinement of all non-hydrogen atoms with anisotropic thermal parameters, and with all organic hydrogen atoms included in fixed positions, peaks corresponding to the expected positions of the three iridium-bound hydrogen atoms were found as three of the top four peaks on the map. The three hydrogen atoms were refined with isotropic thermal parameters, keeping all other hydrogen atoms fixed in idealized geometries with assigned thermal parameters 1–2  $\text{\AA}^2$  larger than the equivalent  $B_{\text{iso}}$  of the carbon to which they were attached. Refinement converged rapidly and cleanly. A secondary extinction coefficient<sup>13</sup> was included in the least-squares refinement after inspection of the low-angle high-intensity data indicated a necessity for such a correction.

Sources of scattering factors etc. were as given for **2**. The  $p$  factor was set to 0.02.

The largest peak in the final difference Fourier map had an electron density of  $0.87 \text{ e}^-/\text{\AA}^3$  and was located near the iridium atom.

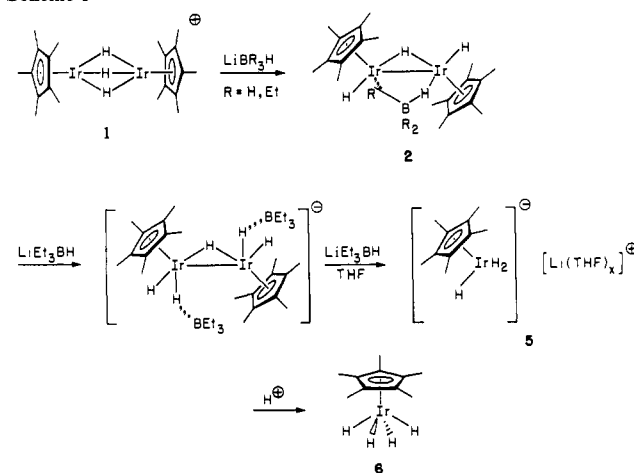
The final residuals for 284 variables refined against the 4989 data for which  $F^2 > 3\sigma(F^2)$  were  $R = 1.91\%$ ,  $R_w = 2.41\%$ ,  $R_{\text{all}} = 2.93\%$ , and  $GOF = 1.391$ .

Positional and thermal parameters of the refined atoms are given in Table III. The positions of the unrefined hydrogen atoms and a listing of  $F_o$  and  $F_c$  are available as Supplementary Material.

**Table III.** Positional Parameters and Their Estimated Standard Deviations for **9c**<sup>b</sup>

atom	x	y	z	$B, \text{\AA}^2$
Ir(1)	0.09033 (1)	0.42880 (1)	0.21483 (1)	3.486 (2)
Sn(1)	0.12538 (2)	0.66442 (2)	0.28823 (2)	3.314 (4)
C(1)	0.2797 (3)	0.3554 (3)	0.1528 (3)	4.47 (7)
C(2)	0.1664 (4)	0.2614 (3)	0.1254 (3)	4.48 (7)
C(3)	0.1298 (4)	0.2405 (3)	0.2314 (3)	5.09 (8)
C(4)	0.2208 (4)	0.3233 (3)	0.3216 (3)	4.90 (7)
C(5)	0.3135 (3)	0.3940 (3)	0.2732 (3)	4.63 (7)
C(6)	0.3633 (4)	0.3977 (4)	0.0702 (3)	6.6 (1)
C(7)	0.1068 (5)	0.1869 (4)	0.0077 (4)	6.8 (1)
C(8)	0.0232 (5)	0.1406 (3)	0.2416 (4)	7.7 (1)
C(9)	0.2257 (5)	0.3273 (4)	0.4466 (3)	7.8 (1)
C(10)	0.4344 (4)	0.4828 (4)	0.3381 (4)	7.2 (1)
C(11)	-0.0666 (3)	0.7447 (3)	0.3014 (2)	3.78 (6)
C(12)	-0.1949 (4)	0.6806 (3)	0.2510 (3)	4.82 (8)
C(13)	-0.3164 (4)	0.7375 (4)	0.2516 (3)	5.89 (9)
C(14)	-0.3107 (4)	0.8573 (4)	0.3049 (4)	6.10 (9)
C(15)	-0.1863 (4)	0.9224 (3)	0.3586 (4)	6.6 (1)
C(16)	-0.0659 (4)	0.8664 (3)	0.3557 (3)	5.10 (8)
C(17)	0.2458 (3)	0.7237 (3)	0.4579 (2)	3.71 (6)
C(18)	0.1978 (3)	0.6844 (3)	0.5474 (3)	4.46 (7)
C(19)	0.2696 (4)	0.7203 (4)	0.6574 (3)	5.37 (9)
C(20)	0.3915 (4)	0.7954 (4)	0.6794 (3)	5.58 (9)
C(21)	0.4438 (4)	0.8359 (3)	0.5920 (3)	5.39 (9)
C(22)	0.3712 (4)	0.7994 (3)	0.4812 (3)	4.52 (7)
C(23)	0.2288 (3)	0.7654 (3)	0.1827 (2)	3.83 (6)
C(24)	0.2486 (4)	0.7076 (3)	0.0752 (3)	4.93 (8)
C(25)	0.3034 (4)	0.7723 (4)	0.0023 (3)	6.08 (9)
C(26)	0.3383 (4)	0.8983 (4)	0.0366 (3)	6.64 (9)
C(27)	0.3192 (4)	0.9573 (3)	0.1422 (3)	6.5 (1)
C(28)	0.2653 (4)	0.8915 (3)	0.2148 (3)	4.86 (8)
H(1)	0.055 (3)	0.494 (3)	0.119 (3)	5.4 (8) <sup>a</sup>
H(2)	-0.060 (4)	0.405 (3)	0.170 (3)	6.1 (9) <sup>a</sup>
H(3)	0.007 (3)	0.477 (3)	0.317 (3)	6.0 (9) <sup>a</sup>

<sup>a</sup> Atoms refined with isotropic thermal parameters. <sup>b</sup> Anisotropically refined atoms are given in the form of the isotropic equivalent thermal parameter defined as  $(4/3)[a^2B(1,1) + b^2B(2,2) + c^2B(3,3) + ab(\cos \gamma)B(1,2) + ac(\cos \beta)B(1,3) + bc(\cos \alpha)B(2,3)]$ .

**Scheme I**

## Results and Discussion

Metathesis of  $[(C_5(CH_3)_5)Ir]_2(\mu-H)_3A^{7,8a}$  ( $A = PF_6$  or  $BF_4$ ) (**1**) with  $LiBH_4$  yields the novel borohydride dimer  $[(C_5(CH_3)_5)Ir]_2H_3BH_4$  (**2**) as orange-yellow crystals (Scheme I). Initial characterization of **2** proved ambiguous, as the compound is quite thermally sensitive and difficult to purify. The hydride region of the  $^1H$  NMR suggested **2** to be a dimer with two sets of two terminal iridium-bound hydrogens ( $\delta -14.2, -17.7$ ), with the lower field set probably coupled to a non-hydrogen nucleus as the resonance appeared quite broad, and one hydrogen ( $\delta -17.5$ ) bridging the iridium atoms which was not coupled to the non-hydrogen nucleus. Variable-temperature  $^1H$  NMR demonstrated the low ( $-80^\circ C$ ) temperature pattern to be equivalent to the room temperature pattern, indicating that the hydride ligand site ex-

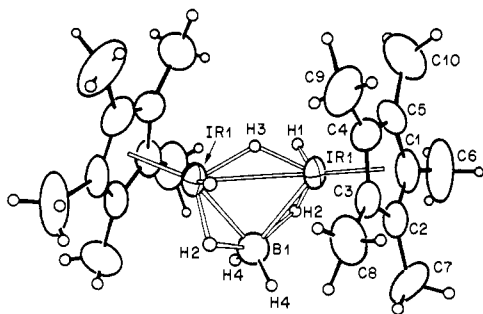


**Figure 1.** ORTEP drawing of **2** (disordered solvent not shown), viewing approximately normal to the Ir–Ir bond vector.

change barrier must be large. Rapid decomposition of **2** occurred at higher temperature, thus removing the possibility of finding the barrier value. Surprisingly, the hydrogen–hydrogen couplings could not be resolved at any temperature, indicating that the coupling constants must be small.

The first suggestion that the non-hydrogen nucleus present was boron resulted from the IR spectrum. In addition to the expected bands due to the  $C_5(CH_3)_5$  ligands, strong bands were observed at 2430, 2360, 2290, 2115, 2040, and 1155  $cm^{-1}$ . The 2115- and 2040- $cm^{-1}$  bands clearly result from terminal Ir–H stretching modes, by analogy with numerous examples from our laboratory.<sup>6a,9</sup> The band at 1155  $cm^{-1}$  we tentatively assign to a mode related to a hydrogen bridging the iridium atoms, based on the broadness of the peak, comparison with the IR spectrum of **3**, and literature data.<sup>8</sup> The very strong bands at 2430, 2360, and 2290  $cm^{-1}$  appear in a region characteristic of B–H stretching frequencies,<sup>14</sup> and little else,<sup>15</sup> strongly suggesting that **2** is a borohydride adduct. Elemental analysis and  $^{11}B\{^1H\}$  NMR confirmed this hypothesis, and an additional resonance ( $\delta$  5.5) in the  $^1H\{^{11}B\}$  NMR spectrum not visible in the uncoupled  $^1H$  NMR spectrum proved that the complex was indeed an iridium borohydride dimer.

However, certain questions remained unanswered at this point. The appearance of *two* resonances in the  $^1H$  NMR ( $\delta$  5.5, –14.2) for borohydride hydrogens implied that the different hydrogens do not rapidly exchange sites, a very uncommon result for the  $BH_4$  ligand.<sup>16</sup> The barriers for such exchanges are known to be low.<sup>14,16</sup> Also, the IR spectra of metal-bound borohydride ligands have been thought to be diagnostic;<sup>14</sup> we were unable to relate the IR bands for **2** to a particular borohydride bonding type.

Because of the ambiguous characterization of **2** and the strong probability of our locating the iridium-bound hydrides crystallographically, we performed a single-crystal X-ray diffraction study. Experimental difficulties and the presence of disordered molecules of pentane in the crystal lattice lowered the experiment's accuracy, but overall a reasonable model of **2** was obtained and shows a surprising bonding mode for the borohydride fragment.

Figure 1 depicts an ORTEP drawing of **2**. A crystallographic twofold axis passes through B(1) and H(3), relating the two halves of the dimer. Each iridium atom is bound to a terminal hydrogen, and a third hydrogen bridges the metals, in agreement with the above predictions. Remarkably, the borohydride ligand bridges both metals as well, a mode well known for carboxylate ligands,<sup>17</sup> but virtually unknown for borohydride. Only one case has been identified and crystallographically characterized previously,<sup>18,19</sup>

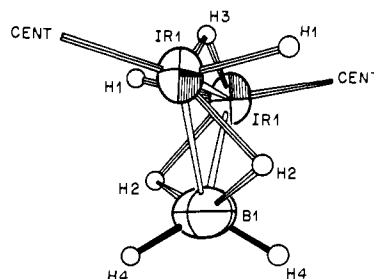
**Table IV.** Selected Bond Distances (Å) and Angles (deg) for  $2 \cdot 1/3 C_5H_{12}$

atom 1	atom 2	distance
Ir(1)	Ir(1)	2.823 (1)
Ir(1)	H(1)	1.47 (8)
Ir(1)	H(2)	1.61 (8)
Ir(1)	H(3)	1.59 (7)
Ir(1)	B(1)	2.214 (4)
Ir(1)	C(1)	2.160 (7)
Ir(1)	C(2)	2.215 (7)
Ir(1)	C(3)	2.259 (6)
Ir(1)	C(4)	2.253 (7)
Ir(1)	C(5)	2.228 (8)
Ir(1)	CENT <sup>a</sup>	1.869
B(1)	H(2)	1.77 (8)
B(1)	H(4)	1.18 (8)

atom 1	atom 2	atom 3	angle
Ir (1)	Ir(1)	CENT	134.3
Ir(1)	Ir(1)	H(1)	89.9 (30)
Ir(1)	Ir(1)	H(2)	86.1 (33)
Ir(1)	Ir(1)	B(1)	50.4 (2)
CENT	Ir(1)	H(1)	128.8
CENT	Ir(1)	H(2)	131.2
CENT	Ir(1)	H(3)	121.9
CENT	Ir(1)	B(1)	126.9
H(1)	Ir(1)	H(2)	60.4 (39)
H(1)	Ir(1)	H(3)	84.2 (50)
H(1)	Ir(1)	B(1)	99.7 (30)
H(2)	Ir(1)	H(3)	106.0 (34)
H(3)	Ir(1)	B(1)	77.5 (23)
Ir(1)	H(3)	Ir(1)	125.8 (57)
Ir(1)	B(1)	Ir(1)	79.21 (24)
Ir(1)	B(1)	H(4)	118.8 (40)
Ir(1)	B(1)	H(4)	107.5 (40)
H(4)	B(1)	H(4)	118.9 (80)
Ir(1)	B(1)	H(2)	45.9 (27)
Ir(1)	B(1)	H(2)	104.0 (30)
H(2)	B(1)	H(2)	145.6 (56)
H(2)	B(1)	H(4)	74.6 (45)
H(2)	B(1)	H(4)	124.4 (49)
Ir(1)	H(2)	B(1)	81.8 (38)

<sup>a</sup> CENT is the calculated centroid of the pentamethylcyclopentadienyl ring.



**Figure 2.** ORTEP drawing of **2**, viewing approximately along the Ir–Ir bond vector. CENT represents the calculated centroid of the pentamethylcyclopentadienyl ring.

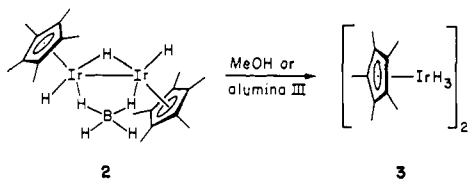
in which two borohydrides each donate three hydrogens to a cobalt dimer. While the positions of the hydrogen atoms in our model are somewhat inaccurate due to the nature of the X-ray diffraction experiment and to the experimental difficulties, the general atomic locations seem sufficient for tentative conclusions to be drawn.

As may be seen from Table IV, the bond lengths and angles for the  $(C_5(CH_3)_5)Ir$  fragments of the molecule lie within the expected ranges for such species; the Ir–Ir distance of 2.823 (1) Å clearly indicates the presence of a metal–metal bond. Bond lengths and angles for the borohydride fragment, however, present problems in defining the exact nature of the molecular interactions. While the average B(1)–H(4) distance (1.18 (8) Å) lies well within

- (14) Marks, T. J.; Kolb, J. R. *Chem. Rev.* **1977**, *77*, 263.  
 (15) Streitwieser, A.; Heathcock, C. H. "Introduction to Organic Chemistry"; MacMillan: New York, 1976.  
 (16) (a) Letts, J. B.; Mazanec, T. J.; Meek, D. W. *J. Am. Chem. Soc.* **1982**, *104*, 3898 and references therein. (b) Takusagawa, F.; Fumagilli, A.; Koetzle, T. F.; Shore, S. G.; Schmitkons, T.; Fratini, A. V.; Morse, K. W.; Wei, C.-Y.; Bau, R. *J. Am. Chem. Soc.* **1981**, *103*, 5165 and references therein. (c) Wink, D. J.; Cooper, N. J. *J. Chem. Soc., Dalton Trans.* **1984**, 1257 and references therein.  
 (17) Cotton, F. A.; Wilkinson, G. "Advanced Inorganic Chemistry", 4th ed.; Wiley and Sons: New York, 1980.  
 (18) Holah, D. G.; Hughes, A. N.; Maciasek, S.; Magnuson, V. R. *J. Chem. Soc., Chem. Commun.* **1983**, 1308.

- (19) Holah, D. G.; Hughes, A. N.; Hui, B. C.; Wright, K. *Can. J. Chem.* **1974**, *52*, 2990. Holah, D. G.; Hughes, A. N.; Hui, B. C.; Kan, C.-T. *Can. J. Chem.* **1978**, *56*, 2552.

Scheme II



expected values, the average B(1)–H(2) distance (1.77 (8) Å) is very long, much longer than the sum of the covalent bonding radii (1.27 Å) for these atoms.<sup>20</sup> However, this value lies well within the sum of the van der Waals contact radii (ca. 2.8 Å)<sup>21</sup> for boron and hydrogen, clearly suggestive of some significant interaction between the atoms. Related to this observation, the Ir–B(1) distance (2.214 (6) Å), while on the longer side of the range of iridium–boron bond lengths,<sup>22</sup> indicates a strong iridium–boron interaction, probably mediated by the presence of the bridging hydrogen. This effect has been remarked on previously.<sup>16b</sup>

While other workers have found bond variations between boron centers and terminal hydrogen atoms and boron centers and bridging hydrogen atoms in transition-metal complexes,<sup>23</sup> the B(1)–H(2) distance is by far the longest reported and nearly eight standard deviations longer than the B(1)–H(4) distance. Also, the small H(2)–B(1)–H(4) angle (74.7 (4.5)°) and the large H(2)–B(1)–H(4) (124 (5)°) angle are quite different from the expected value of 109.5°. Therefore we consider the “BH<sub>4</sub>” moiety to be strongly distorted from a tetrahedral geometry (Figure 2), and view **2** conceptually as a complex in which a hydrogen atom has been nearly transferred from boron to iridium. Presumably the fact that the borohydride fragment bridges two metal centers contributes to the distortion as well.

Reaction of a sample of pure **2** with excess LiEt<sub>3</sub>BH generates (C<sub>5</sub>(CH<sub>3</sub>)<sub>5</sub>)IrH<sub>3</sub>[Li(THF)<sub>x</sub>] (see below) as the major product by <sup>1</sup>H NMR. Apparently the borohydride dimer, while unreactive toward excess LiBH<sub>4</sub>, does react with the more nucleophilic LiEt<sub>3</sub>BH.

Hydrolysis of a solution of **2**, either by reaction with methanol or by filtration through alumina III, yields the neutral, formally iridium(IV) polyhydride dimer [(C<sub>5</sub>(CH<sub>3</sub>)<sub>5</sub>)IrH<sub>3</sub>]<sub>2</sub> (**3**) (Scheme II). This yellow-orange, air-sensitive complex proved much easier to handle and purify than **2**, being less soluble in pentane and more thermally robust, although it too decomposes on continued heating.

Complex **3** may also be isolated, although in low yield, upon column chromatographic hydrolysis of the reaction mixture when dimer **1** reacts with 2 equiv of LiEt<sub>3</sub>BH. The major product of this reaction is (C<sub>5</sub>(CH<sub>3</sub>)<sub>5</sub>)IrH<sub>4</sub> (**6**). In order for any quantity of **3** to be observed in this reaction, no more than 2 equiv of LiEt<sub>3</sub>BH may be used; amounts in excess of this value yield only **6**. However, dimer **3** does not appear to be an intermediate in the production of **6**, as pure **3** is unreactive toward LiEt<sub>3</sub>BH in benzene solution; the dimer is produced intact upon alumina III hydrolysis of this reaction mixture.

Dimer **3**, in addition to the usual spectroscopic techniques, was characterized by reaction with P(CH<sub>3</sub>)<sub>3</sub>, yielding 2 equiv of (C<sub>5</sub>(CH<sub>3</sub>)<sub>5</sub>)Ir(P(CH<sub>3</sub>)<sub>3</sub>)<sub>2</sub>.<sup>9</sup> This reaction proved surprisingly slow at ambient temperature, suggesting a fairly large barrier to nucleophilic attack by phosphine for this system.

Variable-temperature <sup>1</sup>H NMR and IR spectroscopies indicate that the dimer probably adopts a structure with four terminal iridium-bound hydrogens and two hydrogens bridging the metals. The solid-state IR spectrum shows, in addition to the stretches due to the C<sub>5</sub>(CH<sub>3</sub>)<sub>5</sub> ligand, bands at 2120, 1190, and 1120 cm<sup>-1</sup>.

The 2120-cm<sup>-1</sup> band should be assigned to a terminal iridium-hydride stretching mode. Tentatively, we assign the lower frequency bands to modes related to hydrogen atoms bridging the metals based on the broadness of the peaks and by analogy to previous work.<sup>8</sup>

Clearer characterization resulted from the variable-temperature <sup>1</sup>H NMR experiment. At room temperature, only one resonance (δ -14.8) appears in the <sup>1</sup>H NMR in the upfield hydride region, indicating rapid site exchange. Upon cooling to -80 °C, the resonance broadens into the base line, while the C<sub>5</sub>(CH<sub>3</sub>)<sub>5</sub> resonance remains unaffected. At -120 °C, with a field strength of 500 MHz, two new resonances appear, a broad downfield singlet (δ -10.7) and a broad upfield singlet (δ -17.1). Presumably, the hydrogens couple to some extent, but the broadness of each resonance (ca. 35 Hz at half-height) removes the possibility of resolving this coupling. The relative peak areas are 30:2:4 with the C<sub>5</sub>(CH<sub>3</sub>)<sub>5</sub> peak the largest, suggesting that the downfield resonance corresponds to one type of iridium-bound hydrogen, and the upfield resonance to another type. On the basis of van der Waals radii arguments and literature data,<sup>24</sup> we believe that the larger, upfield resonance corresponds to four terminally bound hydrogens and the smaller, downfield resonance to two hydrogens bridging the two metals. We carried out a line shape analysis of the variable-temperature <sup>1</sup>H NMR data (see Appendix, ref 7), assuming that equivalence of the hydrogen atoms obtains as the atoms move from terminal to bridging to terminal positions, that no more than three hydrogen atoms bridge the metal centers at any one time, and that at no time does an iridium have more than two terminal hydrogen ligands (a total of eight exchange permutations). This allowed calculation of the activation parameters ΔH<sup>‡</sup> = 7.35 (7) kcal, ΔS<sup>‡</sup> = 0.2 (0.3) eu, k<sub>298</sub>(extrapolated) = 3.6 (6) × 10<sup>6</sup> s<sup>-1</sup>, and ΔG<sup>‡</sup><sub>298</sub> = 7.26 (3) kcal. The smallness of this value of ΔG<sup>‡</sup> is in keeping with the difficulty in reaching a static limit.

Reaction of 1-PF<sub>6</sub> or 1-BF<sub>4</sub> with the more nucleophilic trialkylborohydride reducing agent LiEt<sub>3</sub>BH yields a dark solution from which the lithium salt of a trihydride anion, (C<sub>5</sub>(CH<sub>3</sub>)<sub>5</sub>)IrH<sub>3</sub>[Li(THF)<sub>x</sub>] (**5**), can be isolated as a strongly THF-solvated material (Scheme I). The deep red-orange complex, while impossible to purify, proved reasonably soluble in hydrocarbon solvents due to the presence of THF. The presence of pentamethyldiethylenetriamine, pmdeta, in the reaction mixture leads to (C<sub>5</sub>(CH<sub>3</sub>)<sub>5</sub>)IrH<sub>3</sub>[Li(pmdeta)] (**8**) in impure form and mediocre yield, due in part to the formation and persistence of an unknown pmdeta/triethylborohydride adduct. Both **8** and **5** react with Ph<sub>3</sub>SnBr to give (C<sub>5</sub>(CH<sub>3</sub>)<sub>5</sub>)IrH<sub>3</sub>SnPh<sub>3</sub> in fair yield.

Spectral characterization of **5** took the form of comparison with the well-characterized salt (C<sub>5</sub>(CH<sub>3</sub>)<sub>5</sub>)IrH<sub>3</sub>[Li(pmdeta)] (**8**), formed by treatment of (C<sub>5</sub>(CH<sub>3</sub>)<sub>5</sub>)IrH<sub>4</sub> (**6**) with *t*-BuLi and pmdeta (see below); we are quite certain of the formulation of **5** based on these comparisons. The <sup>1</sup>H and <sup>13</sup>C{<sup>1</sup>H} NMR experiments provided the most telling comparisons, so we shall discuss the spectra of both compounds here.

In the <sup>1</sup>H NMR of **8**, in addition to the resonances due to sequestering ligand, resonances due to the C<sub>5</sub>(CH<sub>3</sub>)<sub>5</sub> ligand (δ 2.52) and the iridium-bound hydrogen atoms (δ -19.2) appear as broad singlets. Of note is the significant downfield shift of the C<sub>5</sub>(CH<sub>3</sub>)<sub>5</sub> resonance from that of its neutral precursor (C<sub>5</sub>(CH<sub>3</sub>)<sub>5</sub>)IrH<sub>4</sub> (**6**) (δ 1.99). In addition, the hydride resonance shifts upfield nearly four ppm from that in **6** (δ -15.4). In fact, the resonances for **8** are each well shifted from any of the neutral polyhydride complexes we have characterized containing the (C<sub>5</sub>(CH<sub>3</sub>)<sub>5</sub>)Ir fragment, whether monomeric or dimeric. We suggest this result

(20) Huheey, J. E. "Inorganic Chemistry"; Harper and Row: New York, 1978.

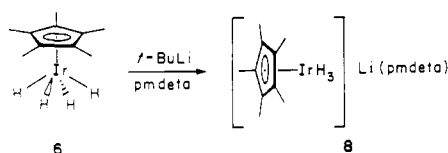
(21) Bondi, A. *J. Phys. Chem.* **1964**, *68*, 441.

(22) Bould, J.; Greenwood, N. N.; Kennedy, J. D.; McDonald, W. S. *J. Chem. Soc., Chem. Commun.* **1982**, 465. Bould, J.; Crook, J. E.; Greenwood, N. N.; Kennedy, J. D.; McDonald, W. S. *Ibid.* **1982**, 346. Crook, J. E.; Greenwood, N. N.; Kennedy, J. D.; McDonald, W. S. *Ibid.* **1981**, 933.

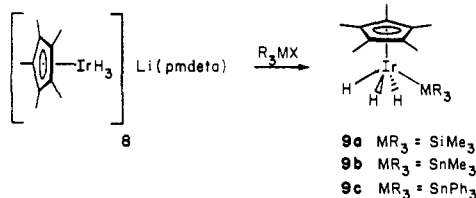
(23) Corey, E. J.; Cooper, N. J.; Canning, W. M.; Lipscomb, W. N.; Koetzle, T. F. *Inorg. Chem.* **1982**, *21*, 192 and references therein.

(24) (a) Only one example of a quadruply hydrogen-bridged metal-metal dimer is known,<sup>24b</sup> which contains sterically undemanding terminal phosphine and hydride ligands; the C<sub>5</sub>(CH<sub>3</sub>)<sub>5</sub> ligands in complex **3** should be much more sterically demanding and should "push" hydrogens to terminal sites. We are attempting to confirm this by growing suitably sized crystals for a neutron diffraction study. (b) Bau, R.; Carroll, W. E.; Teller, R. G.; Koetzle, T. F. *J. Am. Chem. Soc.* **1977**, *99*, 3872. (c) The dimer [(Me<sub>2</sub>PhP)<sub>2</sub>IrH<sub>3</sub>]<sub>2</sub> has been determined to have two bridging and four terminal hydrogen ligands by X-ray diffraction: Robertson, G. B.; Tucker, G. A. *Aust. J. Chem.* **1984**, *37*, 257.

## Scheme III



## Scheme IV



indicates the presence of a very electron-rich (basic) metal center in **8** (cf.  $(C_5(CH_3)_5)Ir(P(CH_3)_3)_2H_2$ <sup>9</sup> [ $^1H$  NMR  $\delta$  2.11 ( $C_5Me_5$ ); -17.4 (Ir-H)] and  $(C_5(CH_3)_5)Ir(P(CH_3)_3)_2HBF_4$ <sup>7</sup> [ $^1H$  NMR  $\delta$  2.09 ( $C_5Me_5$ ); -17.8 (Ir-H)]). For complex **5**, the corresponding resonances occur at  $\delta$  2.18 and  $\delta$  -19.2, respectively, predicting that complexes **5** and **8** are similar in structure and metal basicity.

A similar, and possibly more indicative, result arises from the  $^{13}C\{^1H\}$  NMR spectra of **5** and **8**. For **8**, the  $C_5(CH_3)_5$  ring carbon resonance appears at  $\delta$  85.0, a full 11.5-ppm shift upfield from that of tetrahydride **6**, and the only previous example in our experience<sup>6a,7,9</sup> for these compounds of this resonance lying upfield of  $\delta$  90. For **5**, the corresponding resonance appears at  $\delta$  87.4, strongly suggesting that **5** is a salt of the trihydride anion. The IR spectra of both complexes are consistent with this assignment as well; the band corresponding to the iridium-terminal hydrogen stretch ( $2019\text{ cm}^{-1}$ ) shifts strongly to lower frequency compared to that for tetrahydride **6**, a result noted previously.<sup>25,26</sup>

Compound **5**, like its analogues **7** and **8**, will scavenge a proton from a number of sources to yield tetrahydride **6**, a formal oxidation of an iridium(III) species to an iridium(V) species (Scheme I). It is clear that in the original preparation of **6**, anion **5** was formed in the reaction mixture and converted to **6** when the reaction mixture was filtered through a short column of alumina III. This explains a previously puzzling result: when we attempted to isolate **6** by merely evaporating the solvent from the reaction mixture and subliming the residue, no product ever appeared.

The crystal structure and various reactions of tetrahydride **6** appeared in a communication;<sup>6a</sup> by more careful hydrolysis of the reaction mixture, we have improved the yield to 74% on large-scale syntheses.

Tetrahydride **6** reacts with *t*-BuLi, either with or without the sequestering agent pmdeta, to cleanly generate the anionic trihydride complexes  $(C_5(CH_3)_5)IrH_3Li$  (**7**) and  $(C_5(CH_3)_5)IrH_3\text{-}[Li(pmdeta)]$  (**8**) in good yield and analytical purity (Scheme III). Compound **7** is a somewhat pyrophoric white salt, completely insoluble in inert solvents at ambient temperature, although the isolation of **5** indicates that **7** might be stable in THF solution; so far, our attempts at dissolution have proved unsuccessful.

Complex **8** has the advantage of far greater solubility than **7** and shows no tendency to burn in air. The yellow-white salt decomposes instantly in air to black material, but it may be easily handled under an inert atmosphere. Determination of the molecular weight indicates that the complex is monomeric in solution at ambient temperature, presumably due to the sequestering of the lithium cation by pmdeta. The salt dissolves easily in toluene, benzene, and hexane at ambient temperature without decompo-

Table V. Selected Bond Distances (Å) and Angles (deg) for **9c**.

atom 1	atom 2	distance
Ir(1)	Sn(1)	2.588 (1)
Ir(1)	H(1)	1.50 (3)
Ir(1)	H(2)	1.47 (3)
Ir(1)	H(3)	1.61 (3)
Ir(1)	C(1)	2.248 (3)
Ir(1)	C(2)	2.213 (3)
Ir(1)	C(3)	2.216 (3)
Ir(1)	C(4)	2.251 (3)
Ir(1)	C(5)	2.278 (3)
Ir(1)	Cp(1) <sup>a</sup>	1.890
Sn(1)	C(11)	2.154 (3)
Sn(1)	C(17)	2.166 (2)
Sn(1)	C(23)	2.165 (3)

atom 1	atom 2	atom 3	angle
Cp(1) <sup>a</sup>	Ir(1)	Sn(1)	128.94
Cp(1)	Ir(1)	H(1)	126.6
Cp(1)	Ir(1)	H(2)	128.5
Cp(1)	Ir(1)	H(3)	122.9
Sn(1)	Ir(1)	H(1)	68.9 (11)
Sn(1)	Ir(1)	H(2)	102.5 (12)
Sn(1)	Ir(1)	H(3)	65.8 (11)
H(1)	Ir(1)	H(2)	69.7 (15)
H(1)	Ir(1)	H(3)	110.4 (15)
H(2)	Ir(1)	H(3)	71.9 (16)
Ir(1)	Sn(1)	C(11)	113.80 (7)
Ir(1)	Sn(1)	C(17)	113.86 (7)
Ir(1)	Sn(1)	C(23)	114.57 (7)
C(11)	Sn(1)	C(17)	103.79 (10)
C(11)	Sn(1)	C(23)	104.28 (9)
C(17)	Sn(1)	C(23)	105.41 (10)

<sup>a</sup>Cp(1) is the calculated centroid of the pentamethylcyclopentadienyl ring.

sition or loss of the sequestering agent, allowing homogeneous quenching with stannylating and silylating agents to give new iridium(V) complexes.

Quenching anion **8** (or **7**) with  $Ph_3SnBr$  allows the isolation of the stable iridium(V) trihydride  $(C_5(CH_3)_5)IrH_3SnPh_3$  (**9c**) (Scheme IV). The compound decomposes upon heating to 150 °C in the solid state, and it seems to be air stable both as a solid and in solution. The  $^1H$  NMR of **9c** shows dynamic behavior over the temperature range -65 to 80 °C, allowing the prediction of the molecular structure in solution. At 80 °C, the resonance resulting from the iridium-bound hydrogens ( $\delta$  -15.7) appears as a sharp singlet, with satellite peaks due to the presence of tin ( $^{117}Sn$ , abundance 7.61%;  $^{119}Sn$ , abundance 8.58%; for both isotopes,  $s = 1/2$ ), although the two sets of satellites are unresolved. Near room temperature, the hydride resonance broadens to near the base line, with the tin satellites no longer visible. Decoalescence of the signal occurs at -10 °C; upon cooling the solution to -65 °C, two resonances appear, a downfield doublet ( $\delta$  -15.4) integrating as two hydrogens and an upfield triplet ( $\delta$  -15.6) integrating as one hydrogen. The equivalence of the coupling constants demonstrates that the two sets of hydrogens couple to each other. Although the tin satellites could not be resolved, the most reasonable structure consistent with the data is a "four-legged piano stool", with the  $SnPh_3$  ligand occupying one "leg" site and the hydrogen atoms the other three, giving one hydrogen trans to the tin atom and two hydrogens cis. Such a structure has been predicted previously for  $(C_5(CH_3)_5)Os(CO)H_3$ <sup>27</sup> and observed crystallographically for  $(C_5(CH_3)_5)(C_2H_5)Ru(CO)Br_3$ .<sup>28</sup>

Line shape analysis of the variable-temperature  $^1H$  NMR data (Figure 3), using two exchange permutations (representing each of the cis hydrogens exchanging with the trans hydrogen, but not with each other), yielded activation parameters  $\Delta H^\ddagger = 10.6$  (5) kcal,  $\Delta S^\ddagger = -10.3$  (1.9) eu,  $k_{298}$ (extrapolated) = 297 (15)  $s^{-1}$ , and  $\Delta G^\ddagger_{298} = 13.69$  (3) kcal. The large negative entropy of

(25)  $Cp_2MoH_2/(Cp_2MoHLi)_x$ : D'Aniello, M. J.; Barefield, E. K. *J. Organomet. Chem.* **1974**, *76*, C50. Francis, B. R.; Green, M. L. H.; Luong-Thi, T.; Moser, G. A. *J. Chem. Soc., Dalton Trans.* **1976**, 1339.

(26)  $Cp_2WH_2/[Cp_2WHLi(pmdeta)]_x$ : Cooper, R. L.; Green, M. L. H.; Moelwyn-Hughes, J. T. *J. Organomet. Chem.* **1965**, *3*, 261. Johnson, M. D.; Shriver, D. F. *J. Am. Chem. Soc.* **1966**, *88*, 301. Mink, R. I. Ph.D. Dissertation, University of Illinois, Champaign-Urbana, IL, 1977.

(27) Graham, W. A. G.; Hoyano, J. K. *J. Am. Chem. Soc.* **1982**, *104*, 3722.

(28) Nowell, I. W.; Tabatabaian, K.; White, C. *J. Chem. Soc., Chem. Commun.* **1979**, 547.

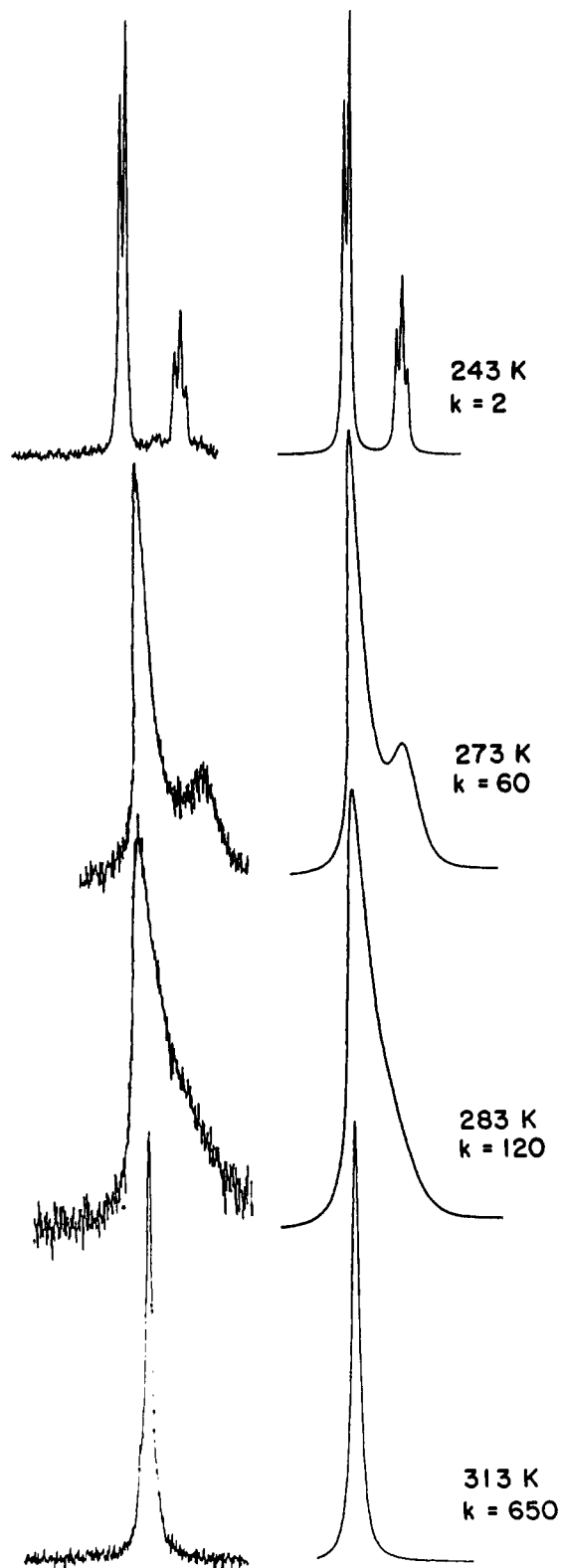


**Figure 3.** Experimental and calculated  $^1H$  NMR spectra (300 MHz) for **9c** at various temperatures. The region shown is that between  $\delta$  -14 and -17.3.

activation seems to correlate with the steric bulk of the non-hydrogen ligand (see below).

In order to test the "piano-stool" hypothesis, we performed a single-crystal X-ray diffraction study of **9c**. Experimental data are given in Table I; an ORTEP view of the molecule appears in Figure 4.

The solid-state result confirms the interpretation of the  $^1H$  NMR. The molecule adopts a nearly perfect piano-stool configuration (given the difference in bonding radii between tin and

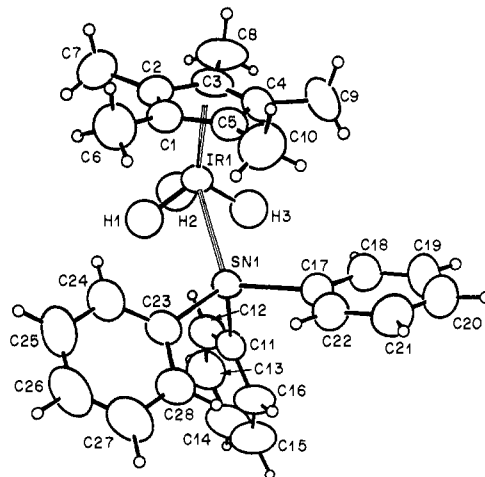


**Figure 4.** ORTEP drawing of **9c**.

hydrogen), minimizing steric contacts between the  $C_5(CH_3)_5$  ring and the ligands. In general, the bond lengths and angles lie in the expected ranges (Table V); within experimental error, the Ir, Sn, and H(2) atoms and the Cp centroid lie in a molecular (not crystallographic) pseudo-mirror plane. Interestingly, a real variation in bond distances from the iridium atom to the  $C_5(CH_3)_5$  ring carbon atoms exists; this effect may be interpreted as either a ring slippage toward the tin atom or a ring tilt away from the tin atom.

The use of  $Me_3SiO_3SCF_3$  or  $Me_3SnCl$  as quenching agents for **8** yields the new complexes  $(C_5(CH_3)_5)IrH_3SiMe_3$  (**9a**) and  $(C_5(CH_3)_5)IrH_3SnMe_3$  (**9b**) as white, crystalline solids which may be sublimed from the reaction mixture. Variable-temperature  $^1H$  NMR experiments indicate that **9a** and **9b** adopt molecular structures isomorphous to that of **9c**; in both cases the low-temperature pattern appears as a doublet integrating as two hydrogens and a triplet integrating as one hydrogen. Interestingly, for these complexes the more upfield resonance is the doublet, whereas for **9c** the more upfield resonance is the triplet. For **9a**, line shape analysis as described above for **9c** yields  $\Delta H^\ddagger = 13.9$  (6) kcal,  $\Delta S^\ddagger = 8.6$  (2.4) eu,  $k_{298}(\text{extrapolated}) = 1.5$  (4)  $\times 10^4$  s $^{-1}$ , and  $\Delta G^\ddagger_{298} = 11.35$  (14) kcal, while for **9b**  $\Delta H^\ddagger = 10.7$  (2) kcal,  $\Delta S^\ddagger = -6.0$  (1.0) eu,  $k_{298}(\text{extrapolated}) = 2.2$  (3)  $\times 10^3$  s $^{-1}$ , and  $\Delta G^\ddagger_{298} = 12.48$  (9) kcal. We note the general decrease in  $\Delta S^\ddagger$  and the resulting increase in  $\Delta G^\ddagger$  as the presumed steric bulk of the silyl/stannyl group increases from  $SiMe_3$  through  $SnMe_3$  to  $SnPh_3$ . Further confirmation of this effect is provided by the even less sterically hindered<sup>29</sup> complex  $(C_5(CH_3)_5)Ir(P(CH_3)_3)H_3BF_4$ ,<sup>7</sup> for which  $\Delta S^\ddagger = 3.7$  (1.6) eu and  $\Delta G^\ddagger_{298} = 10.84$  (8) kcal.

### Conclusion

On the basis of the results outlined in this paper, we propose that the conversion of  $[(C_5(CH_3)_5)Ir]_2(\mu-H)_3^+$  (**1**) to 2 equiv of  $(C_5(CH_3)_5)IrH_4$  (**6**) upon reaction with excess  $LiEt_3BH$  occurs according to the mechanism outlined in Scheme I. Specific features of this hypothesis follow.

Upon reaction of **1** with the first equivalent of borohydride reducing agent ( $LiBH_4$  or  $LiEt_3BH$ ), the neutral, dimeric borohydride complex **2** is produced. When  $LiBH_4$  (R = H, Scheme I) acts as the reducing agent, dimer **2** is unreactive toward further attack by  $LiBH_4$  (it will react further with  $LiEt_3BH$ , however). In this instance, the  $BH_4$  fragment "swings around" and coordinates to both iridium centers, giving the isolated complex studied by X-ray diffraction. When  $LiEt_3BH$  (R = Et, Scheme I) acts as the reducing agent, the borohydride fragment probably does not bridge both metals in the neutral complex **2**, since it is unlikely that the ethyl group can form such a bridge. Instead, the triethyl borohydride anion either fully transfers its hydride to the iridium dimer, yielding transient  $[(C_5(CH_3)_5)IrH_2]_2$  and free triethylborane, or possibly a complex is formed with a hydrogen bridging

(29) Tolman, C. A. *Chem. Rev.* 1977, 313.

the iridium and boron centers and the ethyl groups uncoordinated. In any event, with either borohydride reducing agent, a neutral iridium dimer with at least four coordinated hydrogen atoms is formed.

Hydrolysis of the reaction mixture at this point ( $R = H, Et$ ) by treatment with methanol or chromatography through alumina III generates the polyhydride dimer **3**, presumably by oxidation of the boron center to  $B(OH)_3$  or  $B(OCH_3)_3$  (Scheme II). This dimer represents a dead end in the reaction; **6** cannot be generated by reaction of **3** with  $LiEt_3BH$ .

Further reduction of **2** occurs when  $LiEt_3BH$  acts as the reducing agent (assuming that excess  $LiEt_3BH$  is used), presumably yielding the anionic dimer shown in the scheme. The  $BEt_3$  fragments do not necessarily coordinate as shown; however, no a priori reason exists why they should not, and the presence of boron in **2** and of boron-containing impurities in isolated **5** suggests that " $BEt_3$ " species are not simply inert.

At this point, a third equivalent of  $LiEt_3BH$  splits the anionic dimer into 2 equiv (based on **1**) of monomeric  $(C_5(CH_3)_5)IrH_3[Li(THF)_x]$  (**5**), which we isolated and characterized. This step of the process represents the last in which  $LiEt_3BH$  takes part; thus the formation of **5** from **1** requires 3 equiv of hydride. Experience has shown, however, that somewhat more reducing agent results in higher yields of tetrahydride **6**, probably due to the increased bimolecular reaction rate brought on by larger reactant concentration.

Oxidation of **5** to  $(C_5(CH_3)_5)IrH_4$  (**6**), then, occurs not in the reaction vessel but in the purification procedure. When the reaction mixture is poured through alumina III, impurities and excess  $LiEt_3BH$  are removed; the anionic iridium(III) trihydride monomer **5** is protonated by surface water leading to the neutral iridium(V) tetrahydride **6**. Therefore **6** cannot be isolated from the unhydrolyzed reaction mixture.

The mechanism in Scheme I is very similar to that illustrated in Scheme I in the previous paper.<sup>7</sup> In fact, the molecules in each scheme are isomorphous, with the substitution of  $H^-$  for  $P(CH_3)_3$ . Thus the unisolable monophosphine dimer cation  $[(C_5(CH_3)_5)Ir]_2(P(CH_3)_3)H_3^+$  maps onto borohydride dimer  $[(C_5(CH_3)_5)Ir]_2H_3(BH_4)$  (**2**), the bisphosphine dimer cation  $[(C_5(CH_3)_5)Ir(P(CH_3)_3)(H)]_2(\mu-H)^+$  maps onto the proposed anionic dimer  $[(C_5(CH_3)_5)Ir]_2H_5^-$ , and  $(C_5(CH_3)_5)Ir(P(CH_3)_3)H_2$  maps onto  $[(C_5(CH_3)_5)IrH_3]^-$  (**5**). Protonation of each of the latter leads to the iridium(V) complexes  $(C_5(CH_3)_5)Ir(P(CH_3)_3)H_3^+$  and  $(C_5(CH_3)_5)IrH_4$  (**6**) completing the analogy.

We consider this work to be a particularly detailed study of a hydride-induced reaction which, overall, results in formal oxidation of the metal center.<sup>5</sup> As a referee pointed out, workers in the field know that hydrolysis is often a necessary step after borohydride reduction and that protonation of hydride anions yields polyhydride complexes in which formal oxidation has occurred at the metal center, but this seems to be the first demonstration of the combination of the two concepts in a reaction mechanism.<sup>30</sup> As workers often report hydrolysis or column chromatography of reaction mixtures to destroy the hydridic reducing agent, the potential exists that processes such as described here are general features of polyhydride oxidation chemistry.

Similar potential exists for the formal substitution of hydride anion for phosphine ligands to lead to future chemistry. For example, the stability of the well-studied  $ReH_9^{2-}$  dianion complex<sup>31</sup> might have been expected on the basis of the many complexes of the general form  $ReH_7(PR_3)_2$ , and in fact the formal hydride/phosphine substitution has been applied to this rhenium system.<sup>32</sup> Similarly, applying this substitution to the series  $FeH_2(PR_3)_4$ <sup>33</sup> predicts the stability of  $FeH_6^{4-}$ , an example of which

has been described.<sup>34</sup> We hope that future work in this area will help to develop (or negate) the reasonableness of this phosphine/hydride analogy; one interesting series of complexes which would provide evidence for the hypothesis is the  $WH_{6+x}^{x-}$  group, based on the known  $WH_6(PR_3)_x$  series.<sup>35</sup>

Clearly, the use of  $LiEt_3BH$  is important in the reaction; the nucleophilicity of this reagent must play a role in the formation of **5** (and therefore **6**) from **1**, since different results obtain when  $LiBH_4$  is used. Possibly the inability of the  $Et_3BH^-$  moiety to form stable bridging networks analogous to those of  $BH_4^-$  is a factor as well; however, as **2** reacts with  $LiEt_3BH$  to generate **5**, this factor is of only slight importance. Other workers<sup>36</sup> have commented upon cleaner reactions and higher yields of polyhydrides with use of  $LiEt_3BH$ ; thus the difference observed here appears to be general.

Of importance to the development of iridium(V) chemistry is the synthesis of complexes, **9a**, **9b**, and **9c** by the method described. Green and co-workers<sup>25,26</sup> first employed alkyl lithium reagents to deprotonate organometallic polyhydrides and were able to prepare numerous interesting alkyl, aryl, and acyl hydrides from the anionic species; however, this method has not until now enjoyed widespread use.<sup>7</sup> We have not yet prepared an iridium(V) alkyl hydride, but the syntheses of **9a**, **9b**, and **9c** give hope that such complexes may be isolable. In any event, the work described herein may lead to a general route for the preparation of heteronuclear organometallic polyhydride dimers.

As noted previously,<sup>7</sup> few activation parameter data exist regarding hydride site exchange in organometallic polyhydride species,<sup>37</sup> particularly when the populations of the sites are unequal. For the iridium(V) complexes described, apparently a correlation exists between the values of  $\Delta S^\ddagger$  (and since the enthalpies of activation are similar, of  $\Delta G^\ddagger$ ) and the steric bulk of the non-hydrogen ligand. The results show that when the ligand is bulky, a strong increase in molecular ordering occurs as the transition state is approached, implying that the hydrogen ligands "see" the substituents attached to the silicon or tin as they exchange with one another. How the increase in ordering is actually manifested is unclear; we hope future studies will address this question.

**Acknowledgment.** This work was supported by the Director, Office of Energy Research, Office of Basic Energy Sciences, Chemical Sciences Division, of the U. S. Department of Energy under Contract DE-AC03-76SF00098. We thank Stephen T. McKenna for his assistance in the use of the line-shape program DYNAMAR,<sup>7</sup> and Dr. Richard A. Andersen for helpful discussions regarding complex **2**. The interest of Dr. Earl L. Muetterties in early parts of this work is gratefully acknowledged. The crystal structure analyses were performed at the UC Berkeley X-ray Crystallographic Facility (CHEXRAY); partial funding for the equipment in the Facility was provided by the NSF through Grant No. CHE79-07027.

**Registry No.** 1-PF<sub>6</sub>, 39385-15-4; 1-BF<sub>4</sub>, 96096-80-9; **2**, 96109-61-4; **2**·1/3C<sub>5</sub>H<sub>12</sub>, 96109-62-5; **3**, 96109-63-6; **5**, 96109-64-7; **6**, 86747-87-7; **8**, 96109-66-9; **9a**, 96109-67-0; **9b**, 96109-68-1; **9c**, 96109-69-2;  $(C_5(CH_3)_5)Ir(P(CH_3)_3)H_2$ , 80146-01-6; Ph<sub>3</sub>SnBr, 962-89-0; Me<sub>3</sub>SiO<sub>3</sub>CF<sub>3</sub>, 27607-77-8; Me<sub>3</sub>SnCl, 1066-45-1.

**Supplementary Material Available:** General temperature factor expressions, bond lengths and angles, selected least-squares planes, and listings of  $F_o$  and  $F_c$  for **2**·1/3C<sub>5</sub>H<sub>12</sub> and **9c** (71 pages). Ordering information is given on any current masthead page. This material is also provided on microfilm in the archival edition of the journal, available in many libraries.

(34) Bau, R.; Ho, D. M.; Gibbins, S. G. *J. Am. Chem. Soc.* **1981**, *103*, 4960.

(35) Borisov, A. P.; Makhaev, V. D.; Semenenko, K. N. *Sov. J. Coord. Chem.* **1980**, *6*, 549.

(36) Crabtree, R. H.; Hlatky, G. G. *Inorg. Chem.* **1982**, *21*, 1273.

(37) (a) Meakin, P.; Guggenberger, L. J.; Peet, W. G.; Muetterties, E. L.; Jesson, J. P. *J. Am. Chem. Soc.* **1973**, *95*, 1467. (b) Muetterties, E. L.; Jesson, J. P. In "Dynamic Nuclear Magnetic Resonance Spectra"; Jackman, L. M., Cotton, F. A., Eds.; Academic Press: New York, 1975.

(30) For a recent example of a proposed mechanism similar to that in this paper, see: Davies, S. G.; Moon, S. D.; Simpson, S. J. *J. Chem. Soc., Chem. Commun.* **1983**, 1278.

(31) Abrahams, S. C.; Ginsberg, A. P.; Knox, K. *Inorg. Chem.* **1964**, *3*, 558.

(32) Chatt, J.; Coffey, R. S. *J. Chem. Soc. A* **1969**, 1963.

(33) Gerlach, D. H.; Peet, W. G.; Muetterties, E. L. *J. Am. Chem. Soc.* **1972**, *94*, 4545.